J. Fluid Mech. (1975), *vol.* 68, *part* 1, *pp.* 177–189
Printed in Great Britain

Stability of non-planar shear flow of a stratified fluid

By WILLIAM BLUMEN
Department of Astro-Geophysics, University of Colorado, Boulder

(Received 12 November 1973)

The linear stability of non-planar shear flow of a stably stratified fluid is investigated. Howard's (1961) semicircle theorem, which places bounds on the range of the complex phase speed c, is derived, although sufficient conditions for stability of the (x-directed) basic flow $\bar{u}(y,z)$ have not been established. The stability properties of some particular shear-layer and jet flows for long-wave disturbances are examined. Much of the effort is directed to delineation of unstable properties of the flow $\bar{u}(y,z) = \tanh y \tanh z$ in terms of c, the wavenumber α and a local form J_0 of the Richardson number. Limiting cases are inflexion-point instability ($J_0 = \infty$) and two-dimensional instability of a vertically stratified shear flow ($J_0 < \frac{1}{4}$). The present numerical computations reveal that at least two modes of instability are present for each pair of values of α and J_0 for $\alpha \leqslant 0{\cdot}2$ and $J_0 < \frac{1}{4}$. The source of instability for each mode is examined by means of computed energy transformations. However, numerical difficulties prevent a detailed examination of these unstable modes for $\alpha > 0{\cdot}2$.

1. Introduction

The stability of non-planar parallel shear flow of a stratified fluid is not without interest in the fields of meteorology and oceanography. Although much has been learned about the stability properties of atmospheric and oceanic flows from theoretical and laboratory models of plane parallel shear flows, most geophysical flows are non-planar even to a first approximation. The relative success of modelling geophysical flows by planar representations is generally related to the fact that the principal energy source for disturbance growth resides in the basic shear associated with either the vertical or the horizontal direction.

Pedlosky (1964*a*, *b*) has examined the stability of a non-planar shear flow to quasi-geostrophic wave disturbances. However, little is known about the stability of non-planar parallel flow of a stratified fluid when quasi-geostrophic theory is inapplicable, as is the case, for example, in the vicinity of intense jet streams. The principal difficulties are both analytical and numerical. First, some stability theorems developed for homogeneous shear flow cannot be directly applied and, second, the numerical problem reduces to finding the eigenvalues of a partial differential equation with non-constant coefficients. In the latter circumstance, the numerical analysis and computer capabilities lead to more serious difficulties than are usually met in the eigenvalue problem associated with

planar shear flow or the problem posed by quasi-geostrophic disturbances in non-planar flow.

In the present paper, only linear stability properties of non-planar parallel flows of a hydrostatic and non-rotating fluid will be investigated. The restriction to long-wave perturbations overcomes certain analytical and numerical difficulties and makes it possible to determine some quantitative features of the instability associated with the non-planar character of the basic flow. Although this restriction limits the geophysical application of the results, the present work does provide a foundation for extensions to the non-hydrostatic problem.

Section 2 contains the basic equations and a presentation of some analytical results. In § 3 neutral curves for various shear profiles are presented while some unstable eigenvalues and associated energy transformations appear in § 4. Some final remarks are made in § 5. The interested reader will find in the appendix a brief discussion of the numerical techniques employed.

2. Formulation and theory

Theoretical and numerical results derived from the present model represent an extension of an analysis presented earlier (Blumen 1971*b*, hereafter referred to as I). A Boussinesq model is employed in which the basic state is a non-planar steady parallel flow $\bar{u}(y^*, z^*)$ directed along the x^* axis. In a Cartesian frame, x^* and y^* are directed to the east and north respectively, while z^* is the height. A basic state of hydrostatic balance prevails. The perturbation velocity superposed upon this state is (u^*, v^*, w^*). The thermodynamic variables are the pressure p^*, density ρ^* and temperature T^*. t^* denotes time.

A velocity scale U and length scales L and H, characteristic of the amplitude and the horizontal and vertical variation of the basic zonal shear flow, are introduced for the purpose of non-dimensionalization. As a consequence we take

$$\left.\begin{aligned} (x^*, y^*) &= L(x, y), \quad z^* = Hz, \quad t^* = Lt/U, \\ (\bar{u}^*, u^*, v^*, w^*) &= U(\bar{u}, u, v, Hw/L), \\ p^*/\bar{\rho}^* &= U^2\pi, \quad T^*/\bar{T}^* = U^2\theta/gH, \end{aligned}\right\} \tag{1}$$

where g is the acceleration due to gravity, assumed constant. The non-dimensional linearized perturbation equations for momentum, mass and energy may be expressed as

$$u_t + \bar{u}u_x + v\bar{u}_y + w\bar{u}_z = -\pi_x, \tag{2}$$

$$v_t + \bar{u}v_x = -\pi_y, \tag{3}$$

$$\delta^2(w_t + \bar{u}w_x) = -\pi_z + \theta, \tag{4}$$

$$u_x + v_y + w_z = 0, \tag{5}$$

$$\theta_t + \bar{u}\theta_x + Jw = 0. \tag{6}$$

The aspect ratio is

$$\delta = H/L \tag{7}$$

and

$$J(z) = g\frac{(\gamma_a - \gamma)/\bar{T}^*}{(U/H)^2}, \tag{8}$$

where γ_a denotes the adiabatic lapse rate and $\gamma = -d\overline{T}^*/dz$ is the mean temperature lapse rate. (For an incompressible fluid, the form of (2)–(6) remains intact, but $\theta \propto \rho^*/\overline{\rho}^*$ and $J(z) = (-g\,d\ln\overline{\rho}^*/dz)/(U/H)^2$.) The parameter $J(z)$ has been referred to as the local Richardson number (e.g. by Drazin & Howard 1966) although the square of the local vertical shear does not appear in the denominator. An alternative definition could be made in terms of the internal Froude number $J^{-\frac{1}{2}}$ but the present form is convenient for later use.

The stability equation for the hydrostatic form of (4) has been derived in I. The stability equation for non-hydrostatic modes takes the form

$$[(\overline{u}-c)^{-2}\,\hat{\pi}_y]_y - \alpha^2\{\hat{\pi}(\overline{u}-c)^{-2} + [(J-(\alpha\delta)^2(\overline{u}-c)^2)^{-1}\,\hat{\pi}_z]_z\} = 0, \tag{9}$$

where

$$\pi = \hat{\pi}(y,z)\,e^{i\alpha(x-ct)}, \tag{10}$$

α denotes the x wavenumber, assumed positive, and the phase speed $c = c_r + ic_i$ is complex. Instability is associated with exponential growth at a relative rate αc_i. Hereafter, the carets will be omitted.

At a rigid boundary the normal velocity component vanishes; at infinity all perturbations are required to vanish. As a consequence of (3), (4) and (6) we obtain

$$\pi_y = 0, \quad y = y_1, y_2, \tag{11a}$$

$$\pi_z = 0, \quad z = z_1, z_2. \tag{11b}$$

Semicircle theorem

In I, the normal-mode approach was used to derive Howard's (1961) semicircle theorem for J = constant. The extension to variable J or to non-hydrostatic modes requires no extra effort when the stability equation is expressed as in (9). Multiplication by π^*, the complex conjugate of π, followed by integration and use of (11) leads to

$$\int_{z_1}^{z_2}\int_{y_1}^{y_2}(\overline{u}-c^*)^2\left\{\frac{|\pi_y|^2+\alpha^2|\pi|^2}{|(\overline{u}-c)^2|^2} + \frac{(\alpha\delta)^2\,|\pi_z|^2}{|J-(\alpha\delta)^2(\overline{u}-c)^2|^2}\right\}dy\,dz$$
$$= \int_{z_1}^{z_2}\int_{y_1}^{y_2}\frac{\alpha^2 J\,|\pi_z|^2}{|J-(\alpha\delta)^2(\overline{u}-c)^2|^2}\,dy\,dz. \tag{12}$$

Howard's (1961) semicircle theorem follows directly from (12). This theorem states that, when $J \geqslant 0$ in the field of flow, "the complex eigenvalue c for any unstable mode must lie inside the semicircle in the upper half-plane which has the range of $\overline{u}$ for diameter".

Static instability

Drazin & Howard (1966, p. 62) established that if the atmosphere is statically unstable everywhere ($J < 0$) then any vertical shear flow $\overline{u}(z)$ will be unstable. The form of (12) is identical with that of equation (5.9) in the paper by Drazin & Howard. It thus follows that the above result may be established for the present case by a similar analysis. Consequently, static instability will always occur in a non-planar shear flow $\overline{u}(y,z)$.

Neutral modes

The two results established above are quite general, applying to arbitrary $J(z)$ and $\bar{u}(y,z)$. However, we shall now restrict attention to long waves for which the wavelength λ is comparable with the horizontal length scale L and the square of the aspect ratio (7) satisfies $\delta^2 \ll 1$. This long-wave approximation implies that $\lambda \to \infty$ with L such that the non-dimensional wavenumber α remains finite. Consistent with this interpretation, we set $\delta = 0$ in (9) and retain the normal-mode expression (10). We consider only profiles of the type

$$\bar{u}(y,z) = g(z)\,h(y) \tag{13}$$

and seek stationary neutral solutions ($c_r + ic_i = 0$). Then, as shown in I, the solution of (9) is separable and may be expressed as

$$\pi(y,z) = \Pi(y)\,P(z). \tag{14}$$

In the present case, where $J = J(z)$, the stability equation gives

$$g^2[P'' - (J'/J)\,P'] + J(\beta^2/\alpha^2)\,P = 0, \tag{15}$$

$$h\Pi'' - 2h'\Pi' - \alpha^2 h[1 - (\beta^2/\alpha^2)\,h^2]\,\Pi = 0, \tag{16}$$

where β^2 is the separation constant. The basic reason for introducing the above simplification is to take advantage of the separability property: the more general form of the stability equation (9) does not appear to be separable.

Neutral solutions associated with four different flows will be presented. In all cases

$$J(z) = J_0 \operatorname{sech}^2 z, \tag{17}$$

where $J_0 = J_0(\alpha, c_i = 0)$ defines the neutral-stability curve in the α, J_0 plane. In addition, some attendant instability properties of the flow represented by case 1 below will be delineated.

3. Neutral solutions

Case 1. $\bar{u} = \tanh y \tanh z$

Michalke (1964) has established that the homogeneous shear flow $h(y) = \tanh y$ in $|y| \leqslant \infty$ is unstable to stationary ($c_r = 0$) modes in the wavenumber range $0 \leqslant \alpha < 1$. These modes are bounded by the neutral mode $\alpha = 1$, $c_r = c_i = 0$. The stability of the flow $g(z) = \tanh z$ with $J(z)$ given by (17), in $|z| \leqslant \infty$, has been examined by Holmboe (Miles 1963). The neutral curve $J_0 = \alpha(1-\alpha)$, shown in figure 1, represents a stability boundary. Stationary ($c_r = 0$) non-hydrostatic disturbances are unstable in the region below this curve. Hazel (1969, 1972) has further established that, as the boundaries are moved in from infinity, the longer wavelengths are destabilized if $\infty > |H| \gtrsim 1{\cdot}2$, where $2H$ represents the boundary separation. A few curves reproduced from Hazel's (1969) numerical results are also presented in figure 1. The neutral points $J_0 = a^2 \leqslant \frac{1}{4}$ on the J_0 axis correspond to the case $\delta = 0$, $h(y) = 1$ in the present model. In this case unstable stationary disturbances are found in the range $0 \leqslant J_0 < a^2$. An interpretation of the

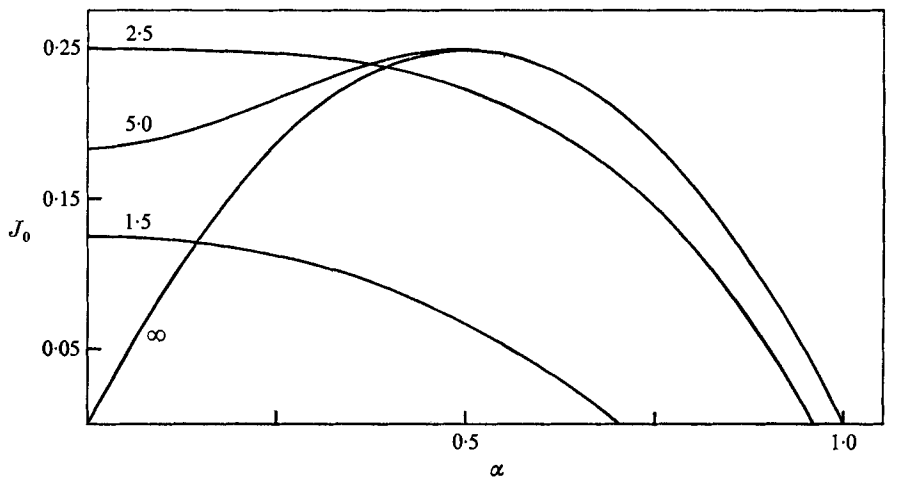

FIGURE 1. Neutral-stability curves for $\bar{u}(z) = \tanh z$, $J = J_0 \operatorname{sech}^2 z$. Each curve is associated with rigid boundaries placed at the indicated distances, $z = |H|$. The unstable region is below each curve.

destabilizing effect of the boundaries for long-wave disturbances may be found in Hazel's papers. We now wish to examine the stability properties of the flow $\bar{u} = \tanh y \tanh z$ of a stratified fluid in which $J(z)$ is given by (17). The previously established results due to Michalke and Hazel will provide useful limiting cases.

We first determine some neutral-stability characteristics by solving (15) and (16). Equation (16) has been solved by Blumen (1970) for $h = \tanh y$. The solution is

$$\Pi = \operatorname{sech}^{\gamma} y, \tag{18}$$

where $\gamma = \alpha^2$ for this case and the separation constant satisfies

$$(\beta/\alpha)^2 = 1 - \alpha^2. \tag{19}$$

Hereafter, it will prove more convenient to deal with the equation

$$W'' + \left[\frac{(1-\alpha^2)J}{g^2} - \frac{g''}{g}\right] W = 0, \tag{20}$$

where the relationship between π and the vertical velocity

$$w(x, y, z) = W(z) (\operatorname{sech} y)^{\alpha^2} \tanh y \, e^{i\alpha(x-ct)} \tag{21}$$

may be determined from (4), (6) and (13). Correspondence between (20) and the Taylor–Goldstein equation, used by Hazel, can be established if $\alpha = 0$ in the latter equation and if $(1-\alpha^2)J$ in (20) is identified with J in the Taylor–Goldstein equation. Then, if $J = J_0 \operatorname{sech}^2 z$ and $g(z) = \tanh z$ are introduced in (20), Hazel's results imply that

$$(1-\alpha^2) J_0 = a^2(H), \tag{22}$$

where $\alpha < 1$. The neutral curve, defining the locus of singular neutral modes in J_0, α space, is displayed in figure 2. The channel width is $2H$, where $H = 2{\cdot}5$. This value of H has been used in the present computations because Hazel has

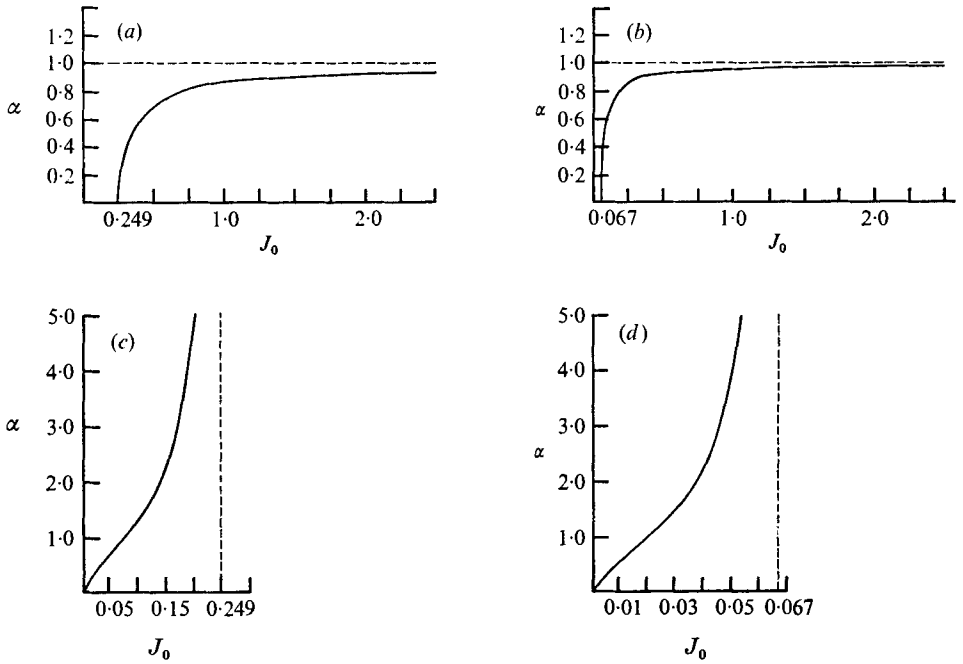

FIGURE 2. Neutral curves for the four profiles in §3. (*a*) Case 1. (*b*) Case 2. (*c*) Case 3. (*d*) Case 4. $J = J_0 \operatorname{sech}^2 z$. In each case $H = 2{\cdot}5$ and $c_r = 0$. The dashed lines are asymptotes.

determined the neutral eigenvalue $J_0 = 0{\cdot}249$ for this separation. Essentially, higher or lower values of H will be associated with lower values of J_0, as shown in figure 1. The eigenfunctions, which are not displayed, must be determined numerically. Instability characteristics of the profile $\bar{u} = \tanh y \tanh z$ are presented in § 4.

Case 2. $\bar{u} = \tanh y \operatorname{sech} z$

Although the instability of the flow $g(z) = \operatorname{sech} z$ has apparently not been delineated, Miles (1963) has established that the stability boundary consists of singular neutral modes for which $c_i = 0$ and $\bar{u}(z) = c_r$ for some z in (z_1, z_2). Since c_r is assumed zero and $\bar{u} \neq 0$ in (z_1, z_2), a stability boundary contiguous to unstable *stationary* modes is not possible. Consequently, the profile $\bar{u} = \tanh y \operatorname{sech} z$ consists of a flow $h = \tanh y$, individually unstable to stationary modes, and a flow $g = \operatorname{sech} z$, which is individually stable to stationary modes.

The neutral curve in J_0, α space may be determined from (20). Upon introduction of (17) and $g = \operatorname{sech} z$, we obtain

$$W'' - [\mu^2 - 2\operatorname{sech}^2 z]\, W = 0, \tag{23}$$

where

$$\mu^2 = 1 + (\alpha^2 - 1) J_0 \geqslant 0. \tag{24}$$

Equation (23) is the same as equation (11) in Howard's (1965) paper. As shown by Howard, there is one positive eigenvalue μ for each value of the separation H greater than the root H_0 of $H_0 \tanh H_0 = 1$ ($H_0 \simeq 1{\cdot}1997$). There is also a discrete spectrum of imaginary eigenvalues μ for any value of H. These correspond, in

the present case, to stable gravity waves. The neutral curve appears in figure 2. The corresponding eigenfunction has been given by Howard.

Case 3. $\bar{u} = \operatorname{sech} y \tanh z$

The stability of the flow $h(y) = \operatorname{sech} y$ has been considered by Blumen (1971*a*). This flow is not unstable to stationary disturbances, but admits a denumerable infinity of stable waves which are solutions to Legendre's equation. As a consequence, we again insert (18) into (16) and find that it is a neutral solution if

$$\gamma = 1 + (1+\alpha^2)^{\frac{1}{2}} \tag{25}$$

and

$$\beta^2 = (1+\alpha^2)^{\frac{1}{2}}[1 + (1+\alpha^2)^{\frac{1}{2}}]. \tag{26}$$

By repeating the analysis presented for case 1, we obtain

$$J_0 = a^2[1 - (1+\alpha^2)^{-\frac{1}{2}}]. \tag{27}$$

This neutral curve is displayed in figure 2.

Case 4. $\bar{u} = \operatorname{sech} y \operatorname{sech} z$

We know that $h(y) = \operatorname{sech} y$ and $g(z) = \operatorname{sech} z$ are individually stable to stationary disturbances. A repetition of previous arguments yields

$$J_0 = (1-\mu^2)[1 - (1+\alpha^2)^{-\frac{1}{2}}]. \tag{28}$$

Application of the semicircle theorem establishes that $c_i = 0$ when $c_r = 0$. As a consequence, the eigenvalues along the curve in figure 2 are associated with stable solutions that are not contiguous to unstable stationary modes.

4. Instability properties

Eigenvalues

A numerical algorithm, described in the appendix, has been used to determine some unstable eigenvalues from (9) with $\delta \equiv 0$. Although (9) is not separable with $c_i \neq 0$, estimates of the unstable eigenvalues in J_0, α space are made by restricting attention to eigenvalues that are adjacent to the neutral curves and for which $c_r = 0$ everywhere. Some obvious drawbacks of this approach are evident. First, unstable regions in which $c_r \neq 0$ are not found. Second, we have not found a truly three-dimensional instability, for example, a destabilization of a profile $\bar{u}(y,z)$ that would be expected to be stable on the basis of the usual inflexion-point and Richardson-number criteria applied to planar flows. Finally, only restricted parameter ranges may be explored because the present numerical scheme becomes unstable. Nonetheless, the present study does provide quantitative information on a class of geophysical flows not previously examined.

Values of some of the unstable eigenvalues associated with the profile $\bar{u} = \tanh y \tanh z$ are summarized in figure 3 and table 1. Two interesting features emerge: instability is not cut off when $J_0 > \frac{1}{4}$ and two unstable stationary modes ($c_r = 0$) occur for each unstable wavenumber α when $J_0 < \frac{1}{4}$. The first result

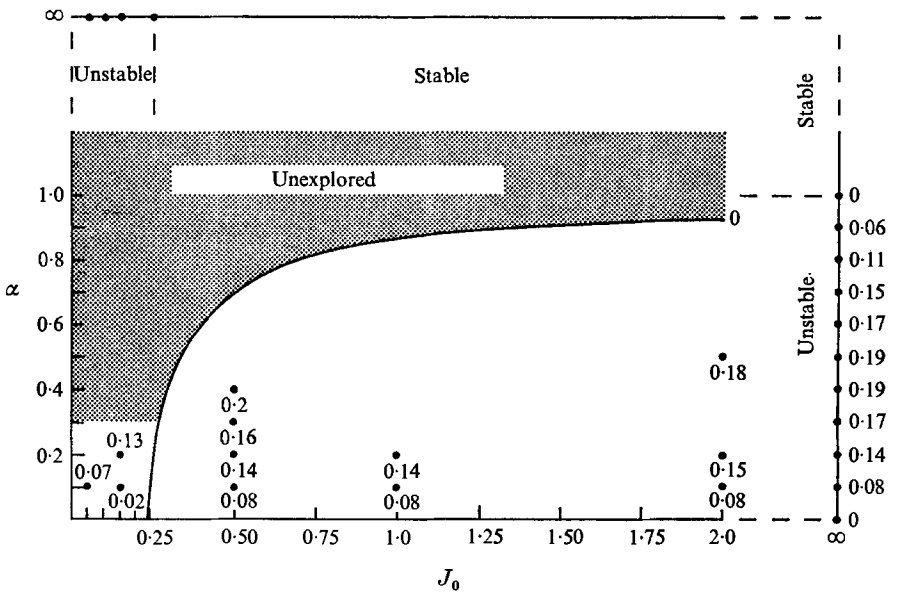

FIGURE 3. Summary of instability characteristics for $\bar{u} = \tanh y \tanh z$, $J = J_0 \operatorname{sech}^2 z$ and stationary ($c_r = 0$) long-wave disturbances. The relative growth rates αc_i are entered at the points where eigenvalues have been determined. The growth rates in the region $J_0 < 0{\cdot}249$ are associated with mode I; those for mode II are slightly smaller as shown in table 1.

J_0 \ α	0·1	0·2	0·3	0·4	0·5	∞†
∞†	0·837	0·697	0·577	0·470	0·375	—
2·0	0·848	0·738	—	—	0·35	—
1·0	0·837	0·719	—	—	—	—
0·5	0·822	0·693	0·55	0·5	—	—
0·15 (I)	0·186	0·647				0·204
0·15 (II)	0·174	0·567				
0·10	—	—				0·289
0·05 (I)	0·74	—				0·367
0·05 (II)	0·67	—				

† 40 grid intervals.

TABLE 1. Eigenvalues c_i ($c_r = 0$). Unless otherwise indicated, 8 grid intervals, $M = N = 8$, have been used in the y and z directions respectively in the determination of these values

is expected because, in the limit as $J_0 \to \infty$, (9) reduces to the π equation associated with homogeneous shear flow. Consequently, the instability occurring to the right of the neutral curve is essentially inflexion-point instability associated with $\tanh y$. This conclusion is borne out by the calculated energy transformations.

The occurrence of two values of $c_i > 0$ for the same J_0 and α is possible because c_i appears in the form of a cubic in (9) or (A 1) (see appendix). Yet, in view of the limited number of grid points used to represent the eigenfunctions ($M = N = 8$) there is a distinct possibility that one of the eigenvalues is spurious, introduced

	$\alpha = 0{\cdot}1$			$\alpha = 0{\cdot}2$		
J_0	R_1	R_2	R_3	R_1	R_2	R_3
2·0	948	0·448	2120	103	0·215	478
1·0	729	0·693	1052	68·3	0·366	186
0·5	342	1·148	298	52·3	0·661	70·2
0·15 (I)	44·0	1·18	37·4	50·3	2·08	24·2
0·15 (II)	29·8	2·61	11·4	10·8	2·52	4·3

TABLE 2. Normalized Reynolds stresses. $R_3 = R_1/R_2$, where R_1 and R_2 are given by equations (32) and (33)

by the numerical scheme. The conjecture that both values are associated with eigenfunctions of (9) will be examined in conjunction with the energy transformations.

Energy transformations

The perturbation kinetic and potential energy equations associated with (2)–(6) are

$$\tfrac{1}{2}\langle u^2+v^2\rangle_t = \langle -(uv\bar{u}_y + uw\bar{u}_z)\rangle + \langle w\theta\rangle, \tag{29}$$

$$\tfrac{1}{2}\langle J^{-1}\theta^2\rangle_t = \langle -w\theta\rangle, \tag{30}$$

where

$$\langle\ \rangle = \int_{z_1}^{z_2}\int_{y_1}^{y_2}\frac{\alpha}{2\pi}\int_0^{2\pi/\alpha}(\ )\,dx\,dy\,dz. \tag{31}$$

As a consequence of the long-wave approximation ($\delta = 0$), $\langle \frac{1}{2}w^2\rangle_t$ does not appear in (29). In order to compare the energy transformations over a range of parameter values we define the following normalized Reynolds stress terms:

$$R_1 = \langle -uv\bar{u}_y\rangle/\langle -w\theta\rangle, \quad R_2 = \langle -uw\bar{u}_z\rangle/\langle -w\theta\rangle. \tag{32), (33}$$

The use of R_1 and R_2 circumvents the introduction of an arbitrary amplitude factor. Moreover, they also provide a convenient measure of the ratio of the rate at which energy is taken out of the mean flow by the Reynolds stresses to the rate at which perturbation kinetic energy is supplied to the available potential energy. Since the problem is linear, a closed energy cycle cannot be described. Consequently, only initial values ($t = 0$) have been calculated. These are presented in table 2.

The influence of inflexion-point instability, as indicated by the magnitude of $R_3 \equiv R_1/R_2$, seems quite evident. The computed relationship between R_3 and J_0 in $0{\cdot}5 \leqslant J_0 \leqslant 2{\cdot}0$ could be anticipated, in view of the limiting result $R_3 \to \infty$ as $J_0 \to \infty$. The values of R_3 for $J_0 = 0{\cdot}15$ still reflect the relative importance of inflexion-point instability because in the parameter range under consideration

$$\alpha^2(\bar{u}-c)^2\,[J^{-1}\pi_z]_z < \pi_{yy}, \tag{34}$$

where the derivatives are of order of magnitude unity in the unstable region.

We did not anticipate the existence of a second mode of instability. However, the evidence suggests that neither of these modes is spurious. First, the shapes of

the computed eigenfunctions for mode I are similar to those computed for $J_0 \geqslant 0{\cdot}5$. This result, in conjunction with the computations of R_3, suggests that mode I is a mode that would exist in the absence of a vertical shear flow in a stably stratified fluid. However, the acceptance of mode II as an eigenfunction of (9) cannot be made on the basis of this information alone. The more persuasive reasons for accepting the reality of mode II are that (i) the sign and magnitude of R_2 indicate an energy transformation associated with unstable vertical shear and (ii) the magnitudes of R_3 associated with mode II are significantly less than the values computed for mode I and the trend is for R_3 to decrease with increasing α. This latter result is in qualitative accord with the problem of planar vertical shear flow, which arises as a limiting case. Let

$$h(y) = \tanh \epsilon^{-1} y, \tag{35}$$

where ϵ is a non-dimensional parameter that characterizes the relative magnitude of the horizontal and vertical shear. Then (22) is replaced by

$$J_0 = a^2[1-(\epsilon\alpha)^2]^{-1}. \tag{36}$$

As $\epsilon \to 0$, $|h| \to 1$ and Hazel's neutral-stability result $J_0 = a^2$ is recovered. In this limiting process the neutral curve, in figure 3, becomes vertical. The instability is wholly confined to the region below $J_0 = a^2$, in accord with the well-known condition for stability, $J_0 \geqslant \frac{1}{4}$. The source of instability for larger values of J_0 is eliminated as the horizontal shear disappears.

We now set $\epsilon \equiv 1$ but permit the static stability to become infinite, to suppress vertical motion. Then, as $J_0 \to \infty$ (a^2 finite), $\alpha \to 1$ from below. The instability of the homogeneous shear flow $h(y) = \tanh y$ is confined to $0 \leqslant \alpha \leqslant 1$. In view of the continuous dependence of the neutral-stability boundary on the model parameters, as limiting cases are approached, the primary source of instability in parameter space is brought more clearly into focus. Yet the interesting aspect of mode II is that it appears to represent a transition from essentially inflexion-point instability to instability of a stratified shear flow, as α increases. In contrast, mode I could be expected to disappear at large α ($J_0 < \frac{1}{4}$).

5. Remarks

The numerical scheme employed here did not prove useful in the delineation of eigenvalues for the profiles of cases 2 and 3, discussed in § 3. Eigenvalues for case 2, $\bar{u} = \tanh y \operatorname{sech} z$, could be determined only for $\alpha \ll 0{\cdot}1$ and $J_0 > 1-\mu^2$. The results (not shown) are in agreement with similar computations made with $\bar{u} = \tanh y \tanh z$ and, as a consequence, establish that inflexion-point instability occurs below the neutral curve in figure 2. This result is plausible, since (24) has the same form as (36) with a^2 replaced by $1-\mu^2$ (> 0). Then the limiting case, inflexion-point instability, may be established in a similar manner.

In order to recover the limiting case associated with $\bar{u} = \operatorname{sech} y \tanh z$, we let

$$h(y) = \operatorname{sech} \epsilon^{-1} y, \tag{37}$$

where $h \to 1$ as $\epsilon \to \infty$. Then in place of (27) we have

$$J_0 = a^2[1-(1+(\epsilon\alpha)^2)^{-\frac{1}{2}}]. \tag{38}$$

$J_0 \to a^2$ as $\epsilon \to \infty$ (α = constant). If the unstable region is wholly contained above the neutral curve in parameter space, then it would appear that the horizontal shear flow exerts a stabilizing influence. However, this conclusion cannot be substantiated because, as shown by Blumen (1971*a*), the limiting case $J_0 = \infty$ exhibits inflexion-point instability with $c_r \neq 0$ in the range $0 \leqslant \alpha < 1{\cdot}465$. Consequently, there is instability to the right of the neutral curve that has not been delineated.

Many questions have been raised by the present study. Perhaps the most interesting speculation concerns general sufficient conditions for stability. Analysis has so far not yielded conditions that are independent of the perturbations themselves. However, for a two-layer model with a continuous profile $\bar{u}(y)$ in each layer, it has been shown (Blumen 1973) that the sufficient conditions may be expressed by the Rayleigh–Fjørtoft condition *and* a bound on the internal Froude number. The latter condition is akin to the requirement that J_0 be greater than 0·5 or 1·0, depending on certain model characteristics.

The numerical results, restricted to a relatively narrow region of parameter space, do not shed light on whether or not both $J \geqslant \frac{1}{4}$ and the inflexion-point criterion are sufficient for stability. This circumstance is not surprising, for Blumen (1971*c*) has shown that stability of a shear flow $\bar{u}(y)$ of a stratified fluid depends on the particular disturbance mode under investigation. However, when inflexion-point instability of $\bar{u}(y)$ does occur some of the available energy from the basic flow must be used to do work against buoyancy. Consequently, the disturbance growth rates are reduced in magnitude. Computations showing this latter effect, for an analogous physical situation, have been presented by Blumen (1970).

The mutual effects of both horizontal and vertical shear are complex, depending on the particular velocity profile, stratification and modes chosen for study. Consequently, it is not possible to state, in general, how the stability of a vertical shear flow will be affected by lateral spatial variations. Drazin (1974) has reached a similar conclusion in his treatment of the vortex-sheet instability of flows with slow lateral variation. Some of the complexities involved in the present model are highlighted by the energy-transformation properties of the modes displayed in table 2. Nevertheless, information on the mutual effects of horizontal and vertical shear would be significant in studies of atmospheric and oceanic jet flows. In the atmospheric case, for example, the value of ϵ in (37) is generally of order 10 or greater. In this situation, we might anticipate small-scale instabilities, such as clear-air turbulence (CAT), to be related to small $J_0 < \frac{1}{4}$ rather than inflexion-point instability. However, in those cases when CAT patches extend over many tens of kilometres, the horizontal shear may be significant.

This research was supported by the Atmospheric Science Section of the National Science Foundation, under Grant GA-31868. Numerical programming was handled by Charles M. Rosenberg and the critical appraisal of the manuscript provided by Dr Philip G. Drazin was both welcome and helpful.

Appendix. Numerical procedures

The unstable eigenvalues $c_i > 0$ ($c_r = 0$) have been determined in the following manner. Finite differences were used to reduce (9) to a system of homogeneous algebraic equations. Then c_i was found by solving the characteristic determinant equation

$$|\mathbf{A} + \mathbf{B}(c_i)| = 0, \tag{A 1}$$

where $\mathbf{A}$ and $\mathbf{B}$ are both complex matrices. Müller's root-finding technique (Conte & deBoor 1972, p. 76) was employed to provide improved estimates of c_i once three distinct approximations to a root of (A 1) had been specified for a particular choice of α, J_0 and profile $\bar{u}(y, z)$. This method, a relatively standard approach, has been recommended for use when reliable initial estimates are available (e.g. Frank 1958; Gersting & Jankowski 1972). Since it is possible to provide good initial estimates of c_i, as discussed in § 4, the root finder behaved in a stable manner when used with determinants as large as order 99.

A standard two-point central differencing procedure was used to represent derivatives. However, in view of the fact that the y region is infinite in all the cases examined, the transformation

$$Y = \sin^{-1}(\tanh y)/\tfrac{1}{2}\pi, \quad |Y| \leqslant 1, \tag{A 2}$$

was introduced. In addition to making the region of integration finite, equal increments ΔY provide greater resolution in the vicinity of the origin than in the tails. This property is highly advantageous because the eigenfunctions in the present class of problems exhibit their greatest variation near $y = Y = 0$.

The accuracy of the algorithm used to solve (A 1) was established by comparison with a test result. Agreement to eight significant figures was attained. Further tests were made to determine the accuracy as a function of the number of grid elements: M along the Y axis and N along the z axis. These tests were made by solving the limiting problems of planar shear flow separately using 40 grid elements in each direction. In each case agreement with Michalke's (1964) and Hazel's (1969) computations was essentially attained. Reduction to 10 and 8 grid elements in each direction established that the unstable eigenvalues could be determined to within an accuracy of better than 10% when $\alpha \leqslant 0{\cdot}2$ and $J_0 \leqslant 2$. However, numerical instabilities led to additional inaccuracies when $\alpha > 0{\cdot}2$. Consequently, the values of c_i displayed in table 1 ($\alpha > 0{\cdot}2$) are less reliable but the trend of changes in $c_i(\alpha)$ is evidently correct.

REFERENCES

Blumen, W. 1970 Shear layer instability of an inviscid compressible fluid. *J. Fluid Mech.* **40**, 769–781.

Blumen, W. 1971*a* Jet flow instability of an inviscid compressible fluid. *J. Fluid Mech.* **46**, 737–747.

Blumen, W. 1971*b* Hydrostatic neutral waves in a parallel shear flow of a stratified fluid. *J. Atmos. Sci.* **28**, 340–344.

Blumen, W. 1971*c* On the stability of plane flow with horizontal shear to three dimensional disturbances. *Geophys. Fluid Dyn.* **2**, 189–200.

BLUMEN, W. 1973 Stability of a two-layer fluid model to nongeostrophic disturbances. *Tellus*, **25**, 12–19.

CONTE, S. D. & DEBOOR, C. 1972 *Elementary Numerical Analysis; an Algorithmic Approach.* McGraw-Hill.

DRAZIN, P. G. 1974 Kelvin–Helmholtz instability of a slowly varying flow. *J. Fluid Mech.* **65**, 781–797.

DRAZIN, P. G. & HOWARD, L. N. 1966 Hydrodynamic stability of parallel flow of inviscid fluid. *Adv. in Appl. Mech.* **9**, 1–89.

FRANK, W. 1958 Computing eigenvalues of complex matrices by determinant evaluation and by methods of Danilewski and Wielandt. *J. Soc. Indust. Appl. Math.* **6**, 378–392.

GERSTING, J. M. & JANKOWSKI, D. F. 1972 Numerical methods for Orr–Sommerfeld problems. *Int. J. Numer. Methods Engng*, **4**, 195–206.

HAZEL, P. 1969 Numerical studies of stratified shear flows. Ph.D. thesis, University of Cambridge.

HAZEL, P. 1972 Numerical studies of the stability of inviscid stratified shear flows. *J. Fluid Mech.* **51**, 39–61.

HOWARD, L. N. 1961 Note on a paper by John W. Miles. *J. Fluid Mech.* **10**, 509–512.

HOWARD, L. N. 1965 The number of unstable modes in hydrodynamic stability problems. *J. Mécanique*, **3**, 433–443.

MICHALKE, A. 1964 On the inviscid instability of the hyperbolic-tangent velocity profile. *J. Fluid Mech.* **19**, 543–556.

MILES, J. W. 1963 On the stability of heterogeneous shear flows. Part 2. *J. Fluid Mech.* **16**, 209–227.

PEDLOSKY, J. 1964*a* The stability of currents in the atmosphere and the ocean. Part I. *J. Atmos. Sci.* **21**, 201–219.

PEDLOSKY, J. 1964*b* The stability of currents in the atmosphere and the ocean. Part II. *J. Atmos. Sci.* **21**, 342–353.